Virtual testing of folding and deployment of composite ultrathin tape spring hinges via unified 2D shell models

IAC-22,C2,2,2,x70003

Virtual testing of folding and deployment of composite ultrathin tape spring hinges via unified 2D shell models

Riccardo Augello[a], Erasmo Carrera[a,b], Alfonso Pagani[a]*, Rebecca Masia[a]

[a] *Mul[2] Group, Department of Mechanical and Aerospace Engineering, Politecnico di Torino, Corso Duca degli Abruzzi 24, 10129, Torino, Italy.* riccardo.augello@polito.it – rebecca.masia@polito.it
[b] *Associazione Italiana di Aeronautica e Astronautica (AIDAA), Italy.* erasmo.carrera@polito.it
* Corresponding Author alfonso.pagani@polito.it

Abstract
This work aims for the study of advanced shell models for the analysis of nonlinear deployable tape-spring hinges. A tape-spring hinge is a combination of thin-walled elastic strips, which results in self-locking hinges that are able to deploy autonomously. The utility of these structures has already been highlighted in a variety of exploration missions for deploying solar panels and antenna systems in a space environment. A numerical tool able to reproduce the real structural behavior of tape spring hinges could represent an advance on this topic. In this context, this work proposes unified shell models for the virtual testing of composite tape-spring hinges by employing Carrera unified formulation and the finite element method. The Newton–Raphson linearization scheme along with a path-following method based on the arc-length constraint is exploited to find the equilibrium path of a tape-spring hinge subjected to coiling bending. The results highlight the accuracy of the proposed approach, comparing the numerical results with those obtained with experiments and literature results and give confidence for further research in this direction.
Keywords: deployable structures; composite shells; tape-spring hinges; Carrera unified formulation; finite element method.

Nomenclature

F_τ	Cross-sectional kinematics
$\boldsymbol{K}_{\boldsymbol{T}}^{ij\tau s}$	Fundamental nucleus of the tangent stiffness matrix
L_{int}	Internal strain energy
M	Number of terms for the given theory approximation order
N_i	Shape functions
$\boldsymbol{u}$	Three-dimensional displacement field
$\boldsymbol{u}_\tau$	Generalized displacements
$\boldsymbol{u}_{\tau i}$	Nodal parameters

Acronyms/Abbreviations

CUF	Carrera Unified Formulation
FEM	Finite Element Method
TSH	Tape-Spring Hinge
DOF	Degrees of Freedom

1. Introduction

Deployable structures made from ultrathin composite materials can be folded elastically and are able to self-deploy by releasing the stored strain energy. They are becoming more widespread because of their lower mass-to-deployed-stiffness ratio, good packaging properties, and lower cost due to a smaller number of component parts and ease of manufacture [1]. Deployable booms found a large number of applications such as for telescopes [2], photovoltaic surfaces [3], antennas [4], solar sails and arrays [4] and advanced aircraft structures [5].

This paper presents a detailed study of a foldable structure such as the Tape-Spring Hinge (TSH). It consists of a thin-walled tube made of carbon-fiber reinforced plastic with an elastically foldable central section made by cutting two longitudinal slots with round ends. This kind of deployable structure is adopted in several space applications, i.e. for the Mars Advanced Radar for Subsurface and Ionosphere Sounding (MARSIS) antenna on the Mars Express spacecraft [6]. TSHs with several design were investigated, for instance a tree-slot TSH, see [7]. Here, the study is focused on a particular hinge design presented in [8] for which, the quasi-static deployment tests were carried out using a bending rig.

For the numerical calculations, the Carrera Unified Formulation (CUF) is recalled. CUF is a generalized framework to generate high order, second generation of theories of structures. By using a recursive index notation, the governing equations of beam, plate and shell structures are written in terms of fundamental nuclei, which are invariant of the theory approximation order. It is coupled with the Finite Element Method (FEM), building mathematical models with high accuracy, see for example [9].

In the present work, the main objective is to further extend CUF to deal with the simulation of TSH made of ultra-thin composite plies with the aim of verifying the model and characterizing the structural behaviour for moderate and large nonlinear states, involving localized and global instabilities. For this purpose, a model based on two-dimensional shell CUF is developed and the results are compared against those from the literature (including numerical and experimental results.

The paper is organized as follows: i) first, the mathematical description of the structural mechanics of the thin TSH boom is described by using a two-dimensional shell CUF-based; ii) second, the nonlinear governing equations are outlined in terms of fundamental nuclei; iii) then, the numerical results are proposed and compared with those from literature; iv) finally, the main conclusions are drawn.

2. Theory and calculation

Figure 1 shows a representative TSH oriented in curvilinear (α, β, z) reference system.

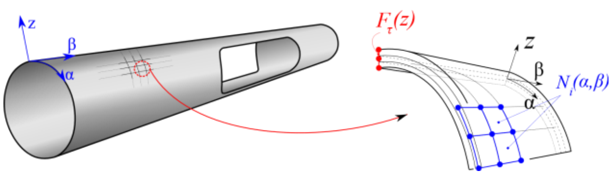

Fig. 1. Representative tape-spring hinge and advanced shell model

Within the framework of the Carrera Unified Formulation (CUF), the three-dimensional displacement field $\boldsymbol{u}(\alpha, \beta, z)$ can be expressed as a general expansion of the primary unknowns. In the case of two-dimensional shell theories, one has:

$$\boldsymbol{u}(\alpha, \beta, z) = F_\tau(z)\boldsymbol{u}_\tau(\alpha, \beta), \tau = 1,2, \dots, M \quad (1)$$

where F_τ are the expansion functions of the coordinates α and β on the middle plane, $\boldsymbol{u}_\tau$ is the vector of the generalized displacements which lay along the shell thickness, M stands for the number of terms used in the expansion, and the repeated subscript τ indicates summation. The choice of F_τ determines the class of the 1D CUF model that is required and subsequently to be adopted. On the other hand, if the Finite Element Method (FEM) is adopted, the generalized displacements are approximated as $\boldsymbol{u}_\tau(\alpha, \beta)=N_i(\alpha, \beta)\boldsymbol{u}_{\tau i}$, where i represents the index summation from 1 to $(p+1)$, p is the polynomial order of the given shape functions N_i, and $\boldsymbol{u}_{\tau i}$ is the vector of nodal parameters.

2.1 Fundamental nuclei for the resolution of nonlinear problems

The nonlinear governing equations corresponding to TSH subjected to large displacements are obtained in this paper by using the principle of virtual displacements as described by Pagani and Carrera [10]. Here, the Newton-Raphson method was employed along with a dedicated arc-length constraint equation, which makes use of the linearized consistent solution.

It can be easily demonstrated that, by using CUF and a recursive notation for the expansion of the kinematics, one can write the equilibrium equations in terms of fundamental nuclei, which are invariant of the theory approximation order. In this manner, in a FEM framework, stiffness arrays can be obtained in an automatic manner with ease and the accuracy of the analysis can be tuned opportunely.

For completeness reasons, we report here the explicit expression of the tangent stiffness matrix. It is obtained by linearizing the virtual variation of the internal strain energy, which holds:

$$d(\delta L_{int}) = \int_V d(\delta \boldsymbol{\varepsilon}^T \boldsymbol{\sigma}) dV$$
$$= \int_V \delta \boldsymbol{\varepsilon}^T d\boldsymbol{\sigma}\, dV + \int_V d(\delta \boldsymbol{\varepsilon}^T)\boldsymbol{\sigma}\, dV \quad (2)$$

where $\boldsymbol{\epsilon}$ and $\boldsymbol{\sigma}$ are the Green-Lagrange strain and the second Piola-Kirchhoff stress vectors respectively, and δ is the virtual variation. If CUF is used along with finite element approximation, and by using the constitutive equations (elastic materials are considered in this work), Eq. (2) becomes:

$$d(\delta L_{int}) = \delta \boldsymbol{u}_{sj}^T \left(\boldsymbol{K}_0^{ij\tau s} + \boldsymbol{K}_{T1}^{ij\tau s} + \boldsymbol{K}_\sigma^{ij\tau s}\right) d\boldsymbol{u}_{\tau i}$$
$$= \delta \boldsymbol{u}_{sj}^T \boldsymbol{K}_T^{ij\tau s}\, d\boldsymbol{u}_{\tau i} \quad (3)$$

where $\boldsymbol{K}_T^{ij\tau s}$ is the fundamental nucleus of the tangent stiffness matrix. According to CUF, this 3x3 matrix, given the cross-section functions F_τ and the 1D shape functions N_i, can be expanded using the indexes τ, s=1,...,M and i, j=1,...,p+1 to obtain the element tangent stiffness matrix of any arbitrarily refined beam model. Note that $\boldsymbol{K}_0^{ij\tau s}$ is the fundamental nucleus of the linear stiffness matrix, $\boldsymbol{K}_{T1}^{ij\tau s}$ is the nonlinear contribution of the fundamental nucleus of the tangent stiffness matrix due to the linearization of the nonlinear constitutive relation, and $\boldsymbol{K}_\sigma^{ij\tau s}$ is the contribution of the geometric stiffness (nonlinear pre-stresses).

The full derivation of the nonlinear problem in the framework of CUF is not given here for the sake of brevity. However, interested readers are referred to the paper of Wu et al. [11].

4. Results

The geometry of the TSH is defined in the deployed configuration and described in [8], and it is shown in Fig. 1. The geometry of the folding section of the tape-spring hinge consists of a 350-mm-long (L) tape springs, separated by 110-mm-long (L_1) with semicircular ends having radius r equals to 15 mm. The internal diameter φ is of 38 mm and a thickness t of 0.2 mm.

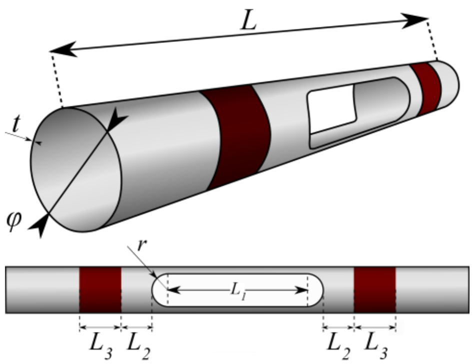

Fig. 2. Geometry of the considered TSH.

The material consists of a layer of weave and the mechanical properties of the cured T300-1k/913 tows and the HexPly 913 resin are defined in Table 1.

Table 1. Properties of cured T300-1k/913 tow and HexPly 913 resin. The Young and shear moduli are expressed in MPa, the density in $\frac{kg}{mm^3}$

Properties	Value
Tow	
E_1	159.520
$E_2 = E_3$	11.660
$G_{12} = G_{13}$	3813
G_{23}	3961
$\nu_{12} = \nu_{13}$	0.27
ν_{23}	0.47
ρ	$1.6 * 10^{-6}$
Resin	
E_m	3390
ν_m	0.41

In the numerical simulation, the weave is simulated as a one-45*-layer with mathematical properties shown in Table 2.

Table 1. Properties of cured T300-1k/913 tow and HexPly 913 resin. The Young and shear moduli are expressed in MPa, the density in $\frac{kg}{mm^3}$

Properties	Value
$E_1 = E_2$	64592.53
E_3	11.660
$G_{12} = G_{13} = G_{23}$	3335
$\nu_{12} = \nu_{13} = \nu_{23}$	0.083
ρ	$1.6 * 10^{-6}$

The holders of the testing machine used to bend the TSH are incorporated within the mathematical model, and they are represented in red in the Fig. 2, where L_2 = 20 mm and L_3 = 22.3 mm. The latter dimensions are not defined in the paper [8], and are calculated according to the figures. A bending moment is applied on both holders, to virtually replicate the experimental setup, and the rotation angle is measured.

2.1 Convergence analysis

As a preliminary study, a convergence analysis on the number of the finite elements is performed. The results are shown in Fig. 3.

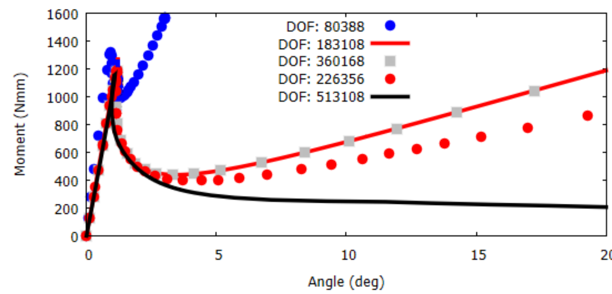

Fig. 3. Convergence analyses.

Clearly, the convergence is not met until the model with 513108 DOF is employed. The peak of the momentum is the same for each model except for the one with 80388 DOF, but the far nonlinear regime is well described by the black line curve. Moreover, the model indicated by the gray boxes makes use of a high-order description of the thickness direction and the same finite element discretization as the solid red line, but no differences arise. We can conclude that, as far as the angle is concerned, we can adopt a linear interpolation for the thickness domain.

2.2 Comparison with literature results

The results coming from the converged model are then compared to those obtained in [8]. In the reference study, the authors used the Abaqus/Explicit simulation technique. The results are shown in Fig. 4.

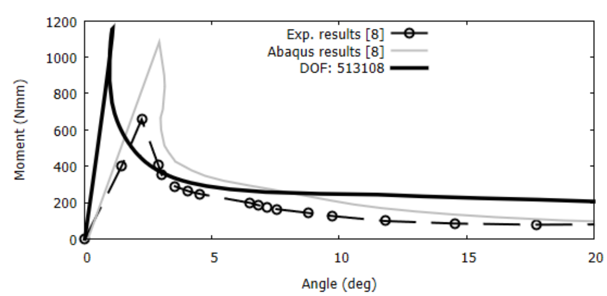

Fig. 4. Comparison with literature results.

Although the overall behavior is clearly described, some differences arise when comparing the obtained results with those from experiments. First of all, the numerical peak is estimated at half of the angle of the experimental one and almost double the applied moment. However, it must be said that in the reference paper the authors made use of two 5-mm-long aluminium rods to model the torsional stiffness of the holders and their torsional constant was tuned so that the simulated angle of snapback was the same as from experiment results. This rods were not included in the present model.

Finally, some of the most important deformed configuration are reported hereafter at 0°, 2° and 12°, respectively:

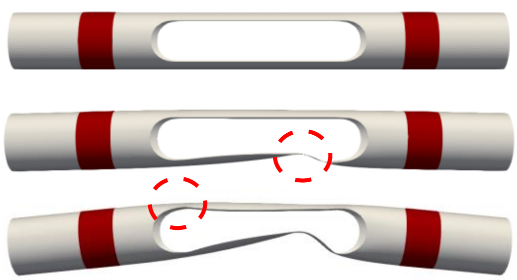

Fig. 5. Deformed configuration at 0°, 2° and 12° respectively.

2.3 Effect of pinching

Each of the previously presented results were obtained pinching the TSH while bending it. In particular, asymmetric pinching was applied to the boom, to enforce the local buckling shown in Fig. 5. A further analysis is made to see the effects of a different application of pinching and how it affects the bending of the TSH, and the results are shown in Fig. 6.

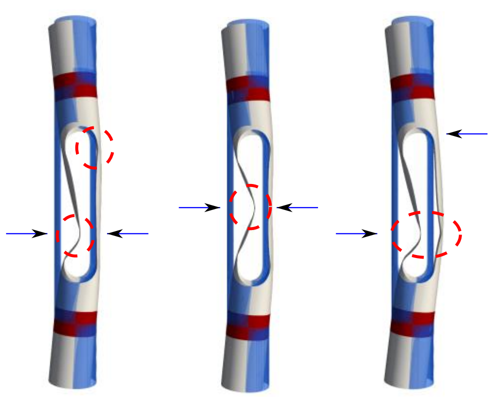

Fig. 6. Effect of different pinching applications

6. Conclusions

This work has explored the use of the two-dimensional model based on the Carrera Unified Formulation (CUF) for simulating the folding of the Tape-Spring Hinge (TSH) boom. The efficacy of the proposed method in describing near and far nonlinear mechanics of the deployable structure was demonstrated by comparing obtained results (with a converged model) to those from literature, including Abaqus/explicit and experiments. The model is able to foresee the local buckling occurring to the deployable and to predict the effects of different pinching applications.

Future work will deal with a dedicated 3D stress analysis and failure identification during the deployment phase.

Acknowledgments

This work is part of a project that has received funding from the European Research Council (ERC) under the European Union's Horizon 2020 research and innovation programme (Grant agreement No. 850437).

References

[1] P. A. Warren, “Foldable Member,” U.S. Patent 374,565 B1, 2002.

[2] L. Blanchard. A tape-spring hexapod for deployable telescopes: Dynamics. In ESA Special Publication, pp. 1-5, 2006.

[3] D. Campbell, R. Barrett, M.S. Lake, L. Adams, E. Abramson, M.R. Scherbarthn, J.S. Welsh, G. Freebury, N. Beidleman, and J. Abbot. Development of a novel, passively deployed roll-out solar array. In 2006 IEEE Aerospace Conference, pp. 1-9, 2006.

[4] M. Leipold, H. Runge, and C. Sickinger. Large SAR membrane antennas with lightweight deployable booms. In 28th ESA Antenna Workshop on Space Antenna Systems and Technologies, ESA/ESTEC, pp. 1-8, 2005.

[5] F. Royer and S. Pellegrino. Ultralight ladder-type coilable space structures. In 2018 AIAA Spacecraft Structures Conference, pp. 1-14, 2018.

[6] D. S. Adams, M. Mobrem, “Lenticular Jointed Antenna Deployment Anomaly and Resolution Onboard the Mars Express Spacecraft,” Journal of Spacecraft and Rockets, Vol. 46, No. 2, 2009, pp. 403–410.

[7] J. C. H. Yee, and S. Pellegrino, “Composite Tube Hinges,” Journal of Aerospace Engineering, Vol. 18, No. 4, 2005, pp. 224–231.

[8] H.M.Y.C. Mallikarachchi, and S. Pellegrino, 2011. Quasi-static folding and deployment of ultrathin composite tape-spring hinges. Journal of Spacecraft and Rockets, 48(1), pp.187-198.

[9] E. Carrera, A. Pagani, and M. Petrolo, 2016. Free vibrations of damaged aircraft structures by component-wise analysis. AIAA Journal, 54(10), pp.3091-3106.

[10] A. Pagani, and E. Carrera, 2018. Unified formulation of geometrically nonlinear refined beam theories. Mechanics of Advanced Materials and Structures, 25(1), pp.15-31.

[11] B. Wu, A. Pagani, W. Q. Chen, and E. Carrera, 2021. Geometrically nonlinear refined shell theories by Carrera Unified Formulation. Mechanics of Advanced Materials and Structures, 28(16), pp.1721-1741